fiers, both using coplanar waveguide transmission lines. Measured gain and return loss data for both amplifiers are shown in Fig. 5.

VII. Stability and Sensitivity of the Amplifier

A distributed amplifier is generally least stable in the vicinity of its cutoff frequency f_c. The addition of positive feedback further destabilizes the amplifier. Therefore the maximum level of positive feedback usable in a given amplifier is limited by the requirement of unconditional stability of the amplifier near its cutoff frequency. It is possible to check for this requirement at the design stage. Another side effect of positive feedback is that it tends to make the amplifier design more sensitive to parameter variations. Distributed amplifiers are known for their general lack of sensitivity to processing parameter variations, resulting in their high processing yield. With positive feedback the high yield can be traded off with amplifier gain.

VIII. Conclusion

Simple expressions were derived giving first-order changes in maximum available gain for an FET with various parallel and series feedback elements. Transition frequencies were established showing that the effect of feedback elements on the stability of an active device can change sign over frequency. It was also shown that the parallel *RC* combination used as series feedback in an FET has a wide-band effect on the available gain of the device. This effect was used in the design of a 2 to 18 GHz distributed amplifier to demonstrate the increased gain that can be achieved over the entire frequency band of the amplifier.

References

[1] Y. Ayasli, R. Mozzi, J. Vorhaus, L. Reynolds, and R. Pucel, "A monolithic GaAs 1–13 GHz traveling wave amplifier," *IEEE Trans. Microwave Theory Tech.* vol. MTT-30, pp. 976–981, July 1982.

[2] M. Rodwell, M. Riaziat, K. Weingarten, and D. Bloom, "Internal microwave propagation and distortion characteristics of travelling wave amplifiers studied by electro-optic sampling," *IEEE Trans. Microwave Theory Tech.* vol. MTT-34, Dec. 1986.

[3] J. Beyer, S. Prasad, R. Becker, J. Nordman, and G. Hohenwarter, "MESFET distributed amplifier design guidelines," *IEEE Trans. Microwave Theory Tech.*, vol. MTT-32, Mar. 1984.

[4] J. M. Rollett, "Stability and power-gain invariants of linear twoports," *IRE Trans. Circuit Theory*, vol. CT-9, pp. 29–32, Mar. 1962.

[5] M. Riaziat, S. Bandy, and G. Zdasiuk, "Coplanar waveguides for MMICs," *Microwave J.*, vol. 30, no. 6, pp. 125–131, June 1987.

Enhanced Through-Reflect-Line Characterization of Two-Port Measuring Systems Using Free-Space Capacitance Calculation

JEFFERY S. KASTEN, STUDENT MEMBER, IEEE, MICHAEL B. STEER, MEMBER, IEEE, AND REAL POMERLEAU

***Abstract*—A through-reflect-line calibration procedure is presented wherein the free-space capacitance and propagation factor of the line standard are used to determine the line characteristic impedance. The method is applied to measurement of a microstrip via.**

Manuscript received March 16, 1989; revised August 29, 1989. This work was supported by BNR through the Center for Communications and Signal Processing, North Carolina State University, Raleigh, NC.

J. S. Kasten and M. B. Steer are with the Center for Communications and Signal Processing, Electrical and Computer Engineering Department, North Carolina State University, Raleigh, NC 27695-7911.

R. Pomerleau is with BNR, 35 Davis Drive, Research Triangle Park, NC 27709.

IEEE Log Number 8932009

I. Introduction

At RF and microwave frequencies the calibration of both vector automatic network analyzers (ANA's) and test fixturing is required to accurately determine the scattering parameters of a device under test (DUT). The most frequently used calibration procedure for noncoaxial measurements is the TRL (through-reflect-line) method [1], which uses as standards a through connection, an arbitrary reflection, and a transmission line of known length and known characteristic impedance Z_c. An approximate determination of Z_c can be made using time-domain reflectometry (TDR); however, TDR cannot determine frequency variations of Z_c. For example, microstrip Z_c can vary by 5 percent from dc to 10 GHz for a typical line [2]. In this paper we present a method of microstrip TRL calibration that uses the calculated free-space capacitance and an experimentally determined propagation constant to determine the frequency-dependent complex characteristic impedance. This impedance is used in the conventional TRL algorithm so that our method is designated enhanced TRL (ETRL).

II. Development of the Method

For uniform TEM transmission lines the characteristic impedance is related to the free-space capacitance and the effective dielectric constant by [3]

$$Z_c = \frac{Z_0}{\sqrt{\epsilon_e}} \tag{1}$$

with

$$Z_0 = \frac{1}{C_0 c} \tag{2}$$

where Z_c is the dielectric-loaded characteristic impedance of the line, Z_0 is its free-space characteristic impedance, C_0 is the free-space capacitance per unit length of the line, c is the velocity of light, and ϵ_e is the effective dielectric constant. Z_c is also related to the propagation constant γ by [4]

$$\epsilon_e = \frac{-\gamma^2 c^2}{\omega^2} \tag{3}$$

where $\gamma = \alpha + j\beta$ is available from measurement as a by-product of the TRL algorithm [5]:

$$\gamma = \frac{\ln\left(\dfrac{A \pm \sqrt{A^2 - 4}}{2}\right)}{l}. \tag{4}$$

Here $A = T11_l \cdot T22_l + T11_l \cdot T22_t - T21_t \cdot T12_l - T12_t \cdot T21_l$. Tij_l and Tij_t are the chain scattering parameters [5] of the line and through calibration standards respectively, and l is the length of the line standard.

Combining (1)–(3) and taking the negative root,

$$Z_c = \frac{j\omega}{c^2 C_0 \gamma} \tag{5}$$

which is used in the standard TRL algorithm as follows. At each frequency, all measurements are transformed from the measurement reference impedance to Z_c so that the inserted line becomes reflectionless. Application of TRL then determines the S parameters of the error network references to Z_c. To complete calibration the S parameters of the error network are returned to the measurement reference impedance system (usually 50 Ω).

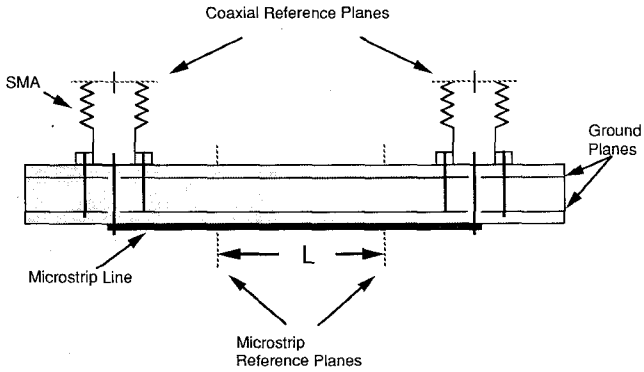

Fig. 1. Printed circuit board measurement fixture. The width of the microstrip line is 8 mils.

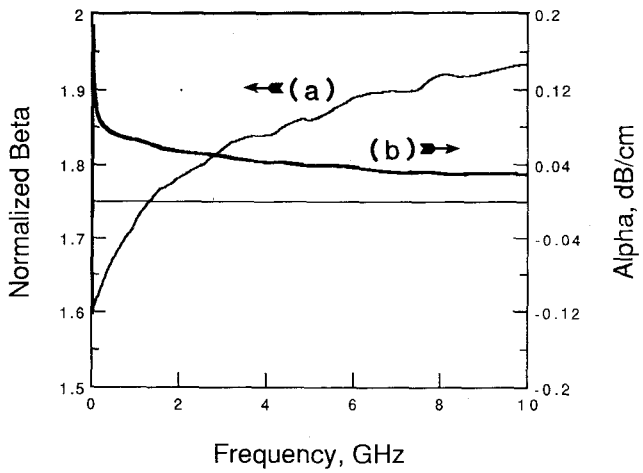

Fig. 2. Complex propagation constant $\gamma = \alpha + j\beta$: (a) normalized $\beta = \beta/\beta_0$ and (b) α in dB/cm.

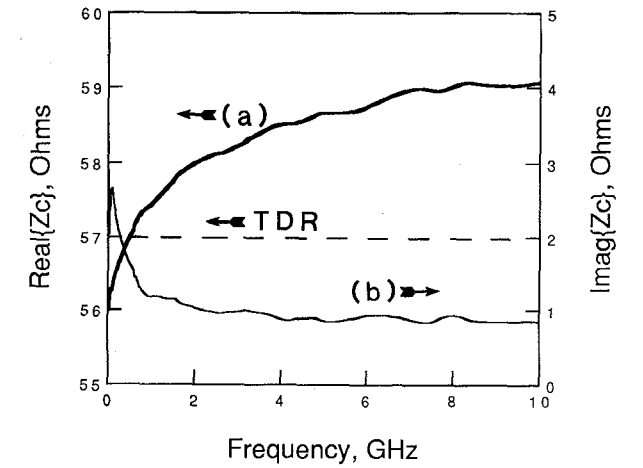

Fig. 3. Microstrip characteristic impedance in Ω: (a) real and (b) imaginary components. Also shown is the characteristic impedance determined using TDR.

III. Results and Discussion

ETRL has been applied to the characterization of discontinuities on printed circuit boards (PCB's). Microstrip lines on PCB's are irregular structures and characteristic impedance models are not available.

Connection to the PCB was made using through-board SMA to microstrip adapters (Fig. 1), and conventional open-short-load

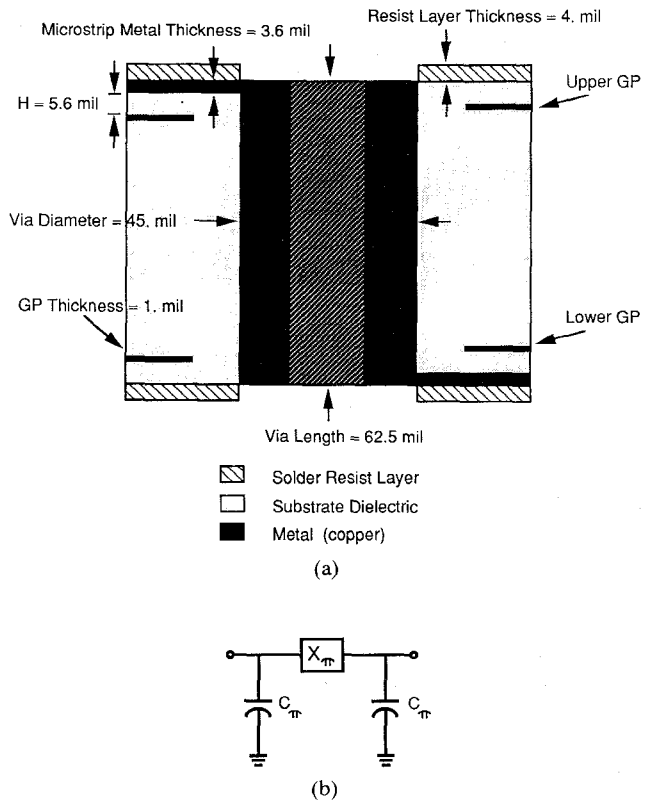

Fig. 4. (a) Cross section and (b) equivalent circuit of a printed circuit board via.

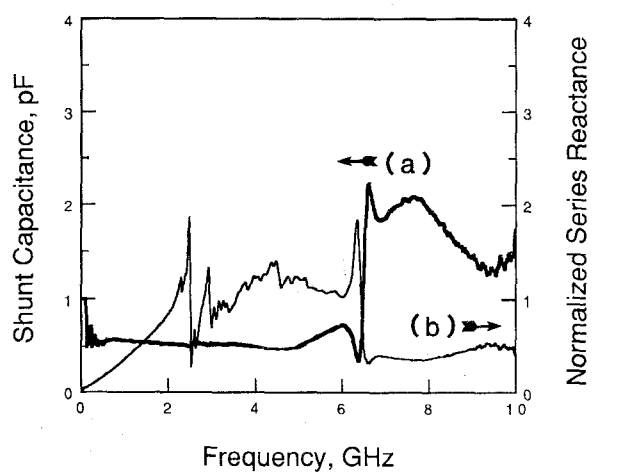

Fig. 5. (a) Via shunt capacitance and (b) series reactance normalized to 50 Ω.

calibration was performed to establish the coaxial reference planes. Substitution of the through ($l = 0$) and line ($l = 2$ in.) measurements in (4) yielded γ as a function of frequency (Fig. 2). Here β has been normalized with respect to a free-space β_0, where $\beta_0 = \omega/c$, to reveal dispersion. Fig. 3 is Z_c calculated using (6), γ, and the free-space capacitance per unit length of the line (the calculation of which is described in [3]).

ETRL was used to characterize the PCB via shown in Fig. 4(a), which has the assumed π equivalent circuit [6] shown in Fig. 4(b). The fit of the de-embedded via measurements to this circuit is shown in Fig. 5. The equivalent circuit is verified at low frequencies as the series element behaves as an inductor and the shunt

elements as a capacitor, but resonances indicate that the PCB via model needs to be modified at frequencies above 2 GHz.

IV. Conclusion

The determination of the characteristic impedance of the TRL standards is important since it directly affects the accuracy of the de-embedded results. The enhancement of TRL presented here incorporates the frequency dependence of the characteristic impedance and includes transmission line loss.

References

[1] G. F. Engen and C. A. Hoer, "Thru-reflect-line: An improved technique for calibrating the dual six-port automatic network analyzer," *IEEE Trans. Microwave Theory Tech.*, vol. MTT-27, pp. 987–993, Dec. 1979.

[2] W. J. Getsinger, "Measurement and modeling of the apparent characteristic impedance of microstrip," *IEEE Trans. Microwave Theory Tech.*, vol. MTT-31, pp. 624–632, Aug. 1983.

[3] I. Bahl and S. Stuchly, "Analysis of a microstrip covered with a lossy dielectric," *IEEE Trans. Microwave Theory Tech.*, vol. MTT-28, pp. 104–109, Feb. 1980.

[4] B. Bianco, L. Panini, M. Parodi, and S. Ridella, "Some considerations about the frequency dependence of the characteristic impedance of uniform microstrips," *IEEE Trans. Microwave Theory Tech.*, vol. MTT-26, pp. 182–185, Mar. 1978.

[5] J. P. Mondal and T-H. Chen, "Propagation constant determination in microwave fixture de-embedding procedure," *IEEE Trans. Microwave Theory Tech.*, vol. 36, pp. 706–714, Apr. 1988.

[6] T. Wang, R. F. Harrington, and J. R. Mautz, "Quasi-static analysis of a microstrip via through a hole in a ground plane," *IEEE Trans. Microwave Theory Tech.*, vol. 36, pp. 1008–1013, June 1988.

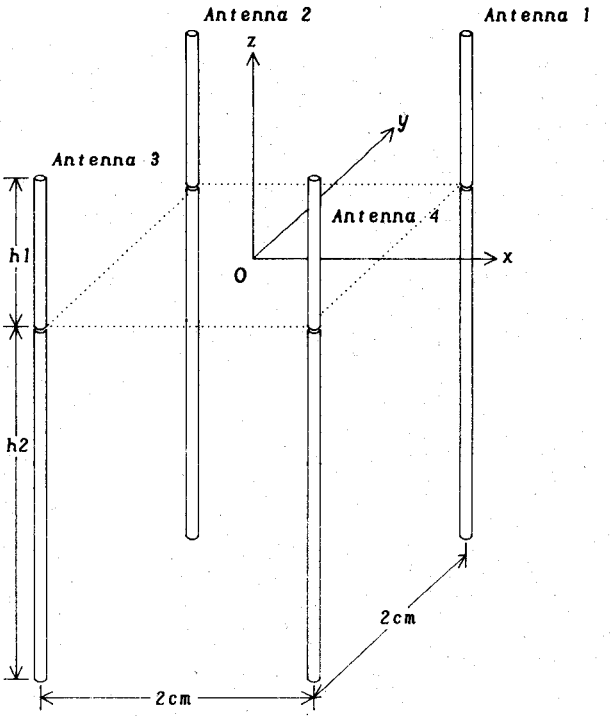

Fig. 1. Square array of four interstitial antennas. The radiating gaps of the antennas are in the lateral plane $z = 0$, and the definition of the coordinates is shown. Details of each antenna are discussed in the text.

Microwave Hyperthermia Induced by a Phased Interstitial Antenna Array

YANG ZHANG, WILLIAM T. JOINES, MEMBER, IEEE, AND JAMES R. OLESON

Abstract—**An interstitial microwave antenna array for hyperthermia cancer treatment is investigated. The purpose is to generate both uniform and controlled nonuniform temperature distributions in biological tissue by modulating the phases of the signals applied to each antenna. The array has four antennas positioned on the corners of a 2 cm square. The distributions of absorbed power within the arrays are computed and then converted into temperature distributions through a heat conduction simulation. The temperature patterns over phantom muscle are presented in both the lateral plane (perpendicular to the antennas) and the axial plane (parallel to the antennas). It has been found that, by proper phase modulation of RF signals applied to each antenna, a uniform heating can be produced in the entire array volume. Also, a peripheral heating pattern may be generated around the array, again by using the proper phase modulation.**

I. Introduction

Microwave-induced hyperthermia has received increased attention in recent years in the treatment of cancer. The primary objective for any hyperthermia treatment is to raise the tumor temperature above 42–43°C for an extended period while keeping the temperature in the surrounding normal tissue well below 43°C. These temperatures can be directly cytotoxic and can potentiate the effect of radiation therapy [1], [2].

A commonly used heating method is interstitial or invasive hyperthermia, where thin coaxial dipole antennas, operating at microwave frequencies (300–2450 MHz), are inserted into the tissue [3]. The antennas are made from coaxial cables that are about 1 mm in diameter and have a radiation gap or gaps in the outer conductor. The antennas are inserted into the tumor through brachytherapy catheters that are nylon tubes about 2 mm in outer diameter used for implantation of iridium for radiation therapy. Through the application of interstitial antennas, various interesting heating patterns may be obtained by using the constructive and/or destructive interference features of the EM fields radiated from the antennas [4], [5]. By changing the driving phase of the signal applied to each antenna, the phase-coherent spot (where constructive interference occurs) may be shifted well away from the center of a 2 cm square array. By varying the relative phase between each antenna, sequentially in time, a more uniform heating pattern may be generated, as well as certain nonuniform heating patterns that may be required for specific applications [6], [7]. In this paper, we investigate the techniques for generating uniform and nonuniform (such as the type in [6] and [7]) heating patterns for a four-antenna array, as shown is Fig. 1. Four interstitial antennas are positioned on the corners of a 2 cm square. The antennas operate at 915 MHz. Theoretical calculations of *SAR* and thermal conduction are performed using properties of phantom muscle tissue. Therefore, the predicted temperature distributions do not represent what they would be in perfused tissue; rather they show what can be accomplished with the phased interstitial antenna arrays when blood flow is neglected.

Manuscript received May 30, 1989; revised September 14, 1989. This work was supported by PHS Grant 1 pol CA 42745-01A1, awarded by the National Cancer Institute, DHHS.

Y. Zhang and W. T. Joines are with the Department of Electrical Engineering, Duke University, Durham, NC 27706.

J. R. Oleson is with the Division of Radiation Oncology, Department of Radiology, Duke University Medical Center, Durham, NC 27710.

IEEE Log Number 8932010.